

Opinion

Potential of the Novel Slot Blot Method with a PVDF Membrane for Protein Identification and Quantification in Kampo Medicines

Takanobu Takata ^{1,2,*} , Togen Masauji ² and Yoshiharu Motoo ^{3,*}

¹ Division of Molecular and Genetic Biology, Department of Life Science, Medical Research Institute, Kanazawa Medical University, Uchinada 920-0293, Ishikawa, Japan

² Department of Pharmacy, Kanazawa Medical University Hospital, Uchinada 920-0293, Ishikawa, Japan; masauji@kanazawa-med.ac.jp

³ Department of Internal Medicine, Fukui Saiseikai Hospital, Wadanakacho 918-8503, Fukui, Japan

* Correspondence: takajjj@kanazawa-med.ac.jp (T.T.); motoo.yoshiharu9082@fukui.saiseikai.or.jp (Y.M.); Tel.: +81-76-286-2211 or +81-76-286-3511 (T.T.); +81-77-623-1111 (Y.M.)

Abstract: Kampo is a Japanese traditional medicine modified from traditional Chinese medicine. Kampo medicines contain various traditional crude drugs with unknown compositions due to the presence of low-molecular-weight compounds and proteins. However, the proteins are generally rare and extracted with high-polarity solvents such as water, making their identification and quantification difficult. To develop methods for identifying and quantifying the proteins in Kampo medicines, in the current study we employ previous technology (e.g., column chromatography, electrophoresis, and membrane chromatography), focusing on membrane chromatography with a polyvinylidene difluoride (PVDF) membrane. Moreover, we consider slot blot analysis based on the principle of membrane chromatography, which is beneficial for analyzing the proteins in Kampo medicines as the volume of the samples is not limited. In this article, we assess a novel slot blot method developed in 2017 and using a PVDF membrane and special lysis buffer to quantify advanced glycation end products-modified proteins against other slot blots. We consider our slot blot analysis superior for identifying and quantifying proteins in Kampo medicines compared with other methods as the data obtained with our novel slot blot can be shown with both error bars and the statistically significant difference, and our operation step is simpler than those of other methods.

Keywords: Kampo medicines; proteins; membrane chromatography; polyvinylidene difluoride membrane; slot blot; tris-(hydroxymethyl)-aminomethane; urea; thiourea; 3-[3-(cholamidopropyl)-dimethylammonio]-1-propanesulfonate; advanced glycation end products



Citation: Takata, T.; Masauji, T.; Motoo, Y. Potential of the Novel Slot Blot Method with a PVDF Membrane for Protein Identification and Quantification in Kampo Medicines. *Membranes* **2023**, *13*, 896. <https://doi.org/10.3390/membranes13120896>

Academic Editor: Laura Donato

Received: 18 October 2023

Revised: 21 November 2023

Accepted: 29 November 2023

Published: 1 December 2023



Copyright: © 2023 by the authors. Licensee MDPI, Basel, Switzerland. This article is an open access article distributed under the terms and conditions of the Creative Commons Attribution (CC BY) license (<https://creativecommons.org/licenses/by/4.0/>).

1. Introduction

Kampo medicine is a Japanese traditional medicine modified and developed based on traditional Chinese medicine from the fifth to the nineteenth centuries [1–3]. Kampo medicines were carefully selected and developed to include various crude drugs (natural products). The traditional Japanese formulation of Kampo remedies influences their selection [2]. Modern Kampo medicines have been produced from extracts using manufacturing methods governed by several national laws in Japan since the late twentieth century [3,4]. They are officially recognized and stipulated in the Japanese Pharmacopoeia, and their quality must comply with legal provisions [3,4]. Considering that the names of Kampo medicines are spelled in Chinese characters and pronounced in Japanese, Japanese researchers have organized the Standards of Reporting Kampo Products (STORK) to assign English names to Kampo medicines [5].

Randomized controlled trials of Kampo medicines have been performed to investigate their clinical effects [6,7]. According to Japanese industry, academia, and government,

applying Kampo medicines for cancer supportive care is the goal for the twenty-first century [8–10]. Despite considerable efforts, the characterization of Kampo medicines' components remains incomplete [11–13]. Analysis of Kampo medicine compounds such as Goshajinkigan and Ninjin'yoeito using three-dimensional high-performance liquid chromatography (3D-HPLC) has detected major low-molecular-weight compounds from the extracts [14–16]. For example, Jin et al. reported the clinical effects of each major low-molecular-weight compound for 34 crude drugs [17]. However, proteins have a high molecular weight. They must be extracted with high-polarity solvents, such as water and 70% ethanol aqueous solution (ethanol: water = 7:3) [18,19], making their solvent removal (evaporation and sublimation) and collection difficult. Moreover, given their relatively suitable concentrations, the proteins in cells or tissue lysates can be readily quantified using the Bradford and bicinchoninic acid (BCA) assays [20,21]. However, these assays may not be appropriate for quantifying protein concentrations in crude drugs. Accordingly, we evaluated the applicability and suitability of conventional technologies for the separation, detection, identification, and quantification of proteins in Kampo medicines [22–24]. We found that, given the insufficient crude sample volume, column chromatography [22,25], electrophoresis [22,26], and enzyme-linked immunosorbent assay (ELISA) [27,28] may be unsuitable for detecting rare proteins within the extract in Kampo medicines. Hence, we focused on membrane chromatography, where samples can repeatedly flow against the membranes, facilitating the collection and separation of proteins [22–24]. Although the membrane material varies and includes cellulose acetate, chitin, chitosan, nylon, and polyvinylidene difluoride (PVDF) [24], we consider that PVDF membrane chromatography is suitable for collecting proteins in Kampo medicines as the PVDF polymer is a strong, semi-crystalline material used in myriad medical instruments (e.g., surgical instruments) [29–32]. PVDF membranes also boast good membrane-forming properties, thermal stability, chemical stability, and mechanical properties [33,34]. Considering that PVDF membranes are often used as filters to produce clean water, natural organic compounds in wastewater, such as proteins and oil, were selected for removal [35,36]. PVDF membranes have also been adopted with the filter blot method for atmospheric particle matter proteins [37] and for electrospray ionization mass spectrometry (ESI-MS) analysis combined with sodium dodecyl sulfate (SDS)–polyacrylamide gel electrophoresis (PAGE) (SDS-PAGE) and “on-PVDF membrane digestion” [38]. In contrast, we focused on slot blot analysis as it is based on the principle of membrane chromatography; however, it requires only a simple and rapid protocol.

In 2017, we developed a novel slot blot analysis and quantified one type of glyceraldehyde-derived advanced glycation end product (AGE): GA-AGEs [39,40]. This method comprises a PVDF membrane and a special lysis buffer for the cell/tissue lysate [39,40]. AGEs are modified proteins formed by interacting with saccharides (e.g., glucose and fructose), their intermediate metabolites/derivatives, and protein [41–43]. PVDF membranes are commonly used to probe proteins in cells or tissues for Western blotting or slot blot analysis [39,40]. Herein, we hypothesized that the novel slot blot method for quantifying AGE-modified proteins could also be used to identify and quantify proteins in Kampo medicines as they share properties with other modified proteins, such as methylated [44–46], acetylated [47–49], phosphorylated [50–52], glycosylated [53–55], and myristoylated [56–58] proteins.

In this article, we compare the performance of our novel slot blot with other commonly used technologies (e.g., column chromatography and electrophoresis) and the other slot blot assay to assess its potential for identifying and quantifying proteins in Kampo medicines.

2. Analysis of Compounds in Kampo Medicines

2.1. Low-Molecular-Weight Compounds in Kampo Medicines, Crude Drugs, and Other Natural Products

Several Kampo medicine crude drugs [1–3] have been analyzed to determine the primary component influencing cellular or organ function. For example, using 3D-HPLC,

Kishida et al. and Nakanishi et al. identified the components of the Goshajinkigan extract, including morroniside, (+)-catechin, loganin, paeoniflorin, penta-*O*-galloylglucose, benzoylmesaconine, cinnamic acid, isoacteoside, benzoylpaeoniflorin, cinnamaldehyde, 16-ketoalisol A, and paeonol [14,16]. Meanwhile, Hosogi et al. identified paeoniflorin, hesperidin, and glycyrrhizic acid as the chemical markers of Ninjin'yoeito extract [16]. Low-molecular-weight compounds are generally extracted using low-polar solvents, such as methanol [10,59], acetone [60], hexane [10,61], and ethyl acetate [61]. These solvents can be evaporated at 40–60 °C, facilitating the facile collection of low-molecular-weight compounds [59–61]. Miyano et al. prepared a water extract of Hangeshashinto and, subsequently, prepared a methanol extract fraction from the water extract, identifying baicalin, glycyrrhizic acid, and berberine [62]; however, this process included a freeze-drying step, which is inconvenient when evaporating low-polar solvents.

2.2. Proteins in Crude Drugs

Proteins in the crude drugs of Kampo medicines have not been thoroughly analyzed against low-molecular-weight compounds. Hence, we introduced previous studies that evaluated challenging proteins in crude drugs, including Yokuinin (*Coix lachryma-jobi* L. var. *Ma-yuen* Stapf.) and Mashinin (*Cannabis Fructus*). Some studies have analyzed low-molecular compounds or polysaccharides that can be extracted into a low-polarity solvent in Yokuinin and investigated their effects in vitro and in vivo [63–69]. However, Li et al. extracted the components in Yokuinin using high-polarity solvents, namely, 0.5 M sodium chloride aqueous, 70% ethanol aqueous, and 12.5 mM sodium borate buffer [18]; these four solvents contained albumin, globulin, prolamin, and glutelin, and their target was glutelin. Due to the high molecular weight of glutelin, Li et al. performed acid hydrolysis of the glutelin and characterized the glutelin peptides using gel filtration chromatography and reversed-phase HPLC (RP-HPLC). Although the low-molecular compounds in *Cannabis* used as crude drugs and commercial product resources for humans have been thoroughly investigated [70–72], their proteins have not. Hence, Liao et al. extracted proteins from *Fructus Cannabis* using water and analyzed them using Fourier transfer infrared (FT-IR) and ultraviolet spectrum (UV) spectroscopy [19]. The proteins were hydrolyzed to obtain various peptides, which were analyzed via liquid chromatography mass spectrometry (LC-MS).

3. Previous and Potential Technologies for the Identification and Quantification of Proteins in Kampo Medicines

High-molecular-weight compounds (>10 kDa), such as proteins and polysaccharides, should be extracted with high-polarity solvents, and samples were performed as the freeze-drying method for water removal [18,19,25]. Certain column chromatography protocols can separate and collect proteins from samples [22–25]. Moreover, silica gel normal phase, reverse normal phase, gel filtration, and ion exchange chromatography have been employed as liquid chromatography methods [25,73,74]. However, the low protein concentration in Kampo medicines may hinder their identification via liquid chromatography. Moreover, if samples undergo a freeze-dry treatment and are injected into the column, the separated proteins must be subjected to another round of freeze-drying [25], thus complicating the overall process. Meanwhile, silica gel normal phase and reverse phase chromatography are unsuitable for separating proteins due to their unstable stationary phases, which cannot be probed with high-molecular-weight compounds [73]. Although researchers can select gel filtration and ion exchange chromatography to separate and collect proteins, the solvent of the mobile phase must be highly polar [73,74]. Additionally, if the solvent used for analysis with gel filtration and ion exchange chromatography contains ions, such as sodium, the samples must be desalted.

Although researchers typically use the Bradford [75,76] or BCA methods [77,78], these require polypropylene tubes and 96-well microplates. When measuring protein concentrations, 100–1000 µL of a sample is required, comprising cell lysate/tissue lysate and

Bradford or BCA reagents. However, the proteins in the water extract of Kampo medicines (or crude drugs) are often low and may be undetectable. When researchers investigate intracellular or tissue proteins *in vitro* or *in vivo*, Western blot with SDS-PAGE [22,26] and ELISA [27,28] are commonly used to identify or quantify the individual proteins (e.g., interleukin-1, tumor necrosis factor- α , and matrix metalloproteinase) [79–81]. The volume of samples and reagents used is 10–30 μ L per SDS-PAGE well and 50–200 μ L per ELISA well. Therefore, individual and rare proteins in Kampo medicines (or crude drugs) are not effectively identified or quantified using these methods.

Membrane chromatography can effectively separate and collect proteins [22–25]. The membrane is used as the stationary phase, while the mobile phase (e.g., liquid or gas) is vertically or parallelly flowed against the membrane. The samples can be continuously run until the collection is complete. If the protein concentration in the samples is low, high sample volumes in the liquid or gas phase can flow repeatedly against the membrane. These membranes primarily comprise cellulose acetate, cellulose/acrylic composite, chitin, chitosan, nylon, and PVDF [24]. Meanwhile, Ogino et al. developed a filter blot method with a PVDF membrane to analyze 3-nitrotyrosine (3-NT)-modified proteins in the atmosphere and compared the results with those obtained using HPLC-electrochemical detection (ECD) (HPLC-ECD) [37]. The 3-NT-modified proteins concentration determined via the filter blot method significantly correlated with that using the HPLC-ECD method ($r = 0.809$, $p < 0.001$). Moreover, Bickner et al. separated proteins with SDS-PAGE, transferred proteins onto PVDF membranes, and performed “on-PVDF membrane digestion.” They then identified proteins with ESI-MS analysis [38]. Although researchers generally perform “in-gel digestion” to identify proteins with ESI-MS or matrix-assisted laser desorption/ionization mass spectrometry (MALDI-MS) [26], “on-membrane digestion” is a high-level technology. Meanwhile, slot blot analysis is based on the principle of membrane chromatography with the sample flowing vertically against the membrane. Therefore, we postulate that slot blot analysis can identify and quantify rare proteins in Kampo medicines. Generally, nitrocellulose or PVDF membranes are selected for the slot blot analysis [25]. Although PVDF has been rarely reported, it offers good membrane-forming properties, thermal stability, chemical stability, and mechanical properties [33,34]. We consider that researchers have favored nitrocellulose membranes because their lysates of cells or tissues are deemed unsuitable for PVDF membranes. However, we have discovered a unique lysis buffer suitable for application with PVDF membranes [24,25].

4. Equipment, Characteristics, and Methodology of the Novel Slot Blot

4.1. Equipment

The novel slot blot method was performed using a Bio-Dot SF Microfiltration Apparatus (Cat. no.: 170-6452; Bio-Rad Laboratories Inc., Hercules, CA, USA) with 48 wells (Figure 1).

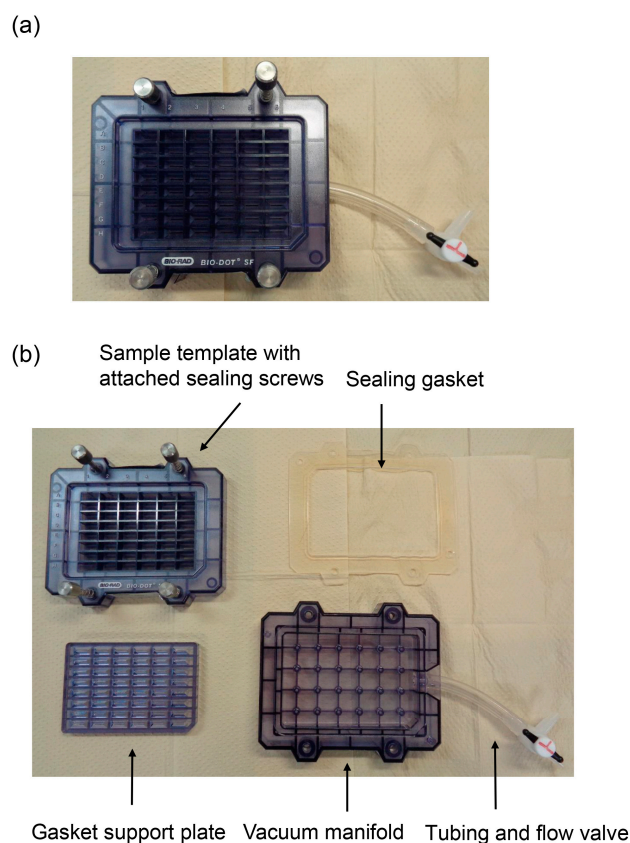


Figure 1. Bio-dot SF microfiltration apparatus (slot blot apparatus with 48 wells). (a) Assembly of the apparatus. (b) Disassembled apparatus.

4.2. PVDF Membrane

The novel slot blot method was performed using a PVDF membrane (Cat. no.: IPVH00010, pore size: 0.45 μm ; Merck Millipore, Darmstadt, Germany). The chemical structure comprised carbon combined with hydrogen and fluorine atoms (Figure 2).

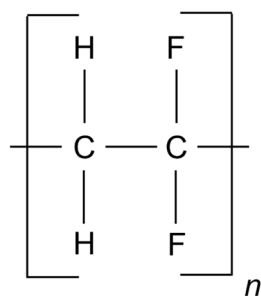


Figure 2. Chemical structure of the PVDF membrane. The “n” indicates that the structure repeated.

Nitrocellulose membranes, not PVDF membranes, are generally used to perform slot blot analysis on various proteins [82–89]. Although protein absorption and PVDF membrane durability are superior [33,34], researchers avoid performing slot blot analysis to identify or quantify proteins. PVDF membranes are commonly used for Western blot analysis [39,40] and can combine with C=O and N–H groups, rendering them superior for protein absorption [33]. However, the appropriate conditions for directly applying protein-containing samples onto a PVDF membrane have not been achieved. Given that electric current transports the proteins during Western blotting, proteins become transferred from the gel to the PVDF membrane. Therefore, the benefits of the PVDF membrane for protein absorption using slot blot can be demonstrated when a superior sample solution is used.

4.3. Lysis Buffer

For our novel slot blot, a custom lysis buffer was produced that differed from commonly used commercial lysis buffers [39,40]. First, tris-(hydroxymethyl)-aminomethane (Tris) (Cat. no.: 011-20095; Fujifilm Wako Pure Chemical, Osaka, Japan), urea (Cat. no.: 217-01215; Fujifilm Wako Pure Chemical), thiourea (Cat. no.: 201-17355; Fujifilm Wako Pure Chemical), and 3-[3-(cholamidopropyl)-dimethylammonio]-1-propanesulfonate (CHAPS) (Cat. no.: 347-04723; Dojindo Laboratories, Kumamoto, Japan) were dissolved in ultrapure water to prepare a solution of 30 mM Tris, 7 M urea, 2 M thiourea, and 4% CHAPS (Solution A, Table 1). Second, a protease inhibitor cocktail tablet (Complete Tablets EDTA-Free, EASY pack, Cat. no.: 04-693-132-001; Roche, Bavaria, Germany) was dissolved in ultrapure water (final volume: 2 mL, Solution B, Table 1 [39,40,90]). Finally, Solutions A and B were mixed (9:1) to form Solution C (Table 1), comprising 27 mM Tris, 6.3 M urea, 1.8 M thiourea, and 3.6% CHAPS. Solution C served as the lysis buffer for our assay [39,90–96]. To create Solution D, Solution B was added to the solution containing Tris, urea, thiourea, and CHAPS in ultrapure water (Table 1) [97–100].

Table 1. Solutions used to prepare the lysis buffer [39,40,90–100].

Solution A	Solution B	Solution C	Solution D
30 mM Tris		27 mM Tris	30 mM Tris
7 M Urea		6.3 M Urea	7 M Urea
2 M Thiourea	1 Protease inhibitor	1.8 M Thiourea	2 M Thiourea
4% CHAPS	cocktail tablet/2 mL	3.6% CHAPS	4% CHAPS
(Ultrapure water)	(ultrapure water)	10% Solution B	4% Solution B
(pH 8.5)		(Ultrapure water)	(Ultrapure water)
		(pH 8.5)	(pH 8.5)

Solution C was prepared following the method described in eight previous studies, and Solution D was prepared following four to quantify intracellular AGEs using the novel slot blot (Table 2). Although PVDF membranes have been previously used in slot blots to quantify proteins, the lysis buffer containing Tris, urea, thiourea, and CHAPS has not been used [101–103]. Gravel et al. used 4 M urea/Tris-buffered saline to quantify influenza type A viral hemagglutinin [103], whereas Papadaki et al. used 8 M urea and 0.1% SDS [104]; these lysis buffers are similar to ours. In contrast, Takino et al. employed a radioimmunoprecipitation (RIPA) buffer for their analysis of large sample concentrations (30 µg of proteins) with their slot blot analysis [39,40,102], whereas our novel method is suitable for samples with small amounts of protein (2.0 µg of proteins). Although RIPA buffer components (e.g., Triton-X) cause denaturation, they may inhibit protein probing onto the PVDF membrane. Papadaki et al. homogenized cardiac tissues with standard rigor buffer containing 1% Triton-X; they then removed the Triton-X and resuspended the pellet in a buffer containing 8 M urea and 0.1% SDS [104], revealing that Triton-X inhibited slot blot analysis.

Table 2. List of references used for preparing Solutions C and D.

Solution	References
C	[39,90–96]
D	[97–100]

Our ideal lysis buffer must promote protein denaturation and not inhibit PVDF membrane probing. When developing this novel slot blot assay, we prepared the lysis buffer based on those selected for two-dimensional electrophoresis (2-DE)-based protein division treatment [39,40]. Meanwhile, many studies have used 7 M urea and 2 M thiourea [105–115] with 2% [109], 3% [105,112], or 4% [106–108,110,111,113] CHAPS. Based

on previous research [113,114], we hypothesized that our lysis buffer promotes protein probing on the PVDF membrane surface. According to McCarthy et al. and Herbert [113,114], urea, thiourea, and CHAPS can denature proteins by acting as chaotropic reagents and surfactants; these reagents disrupt hydrogen bonding and cause protein unfolding, exposing hydrophobic amino acid residues to the solution. CHAPS is combined with urea and thiourea to coat hydrophobic residues and improve solubility, and thiourea/urea combinations are widely used to exploit thiourea's improved denaturing ability [113]. Furthermore, urea may be more important in inhibiting protein probing on the PVDF membrane. Urea reacts with ammonium and cyanate, with cyanate particularly adept at producing isocyanic acid that can subsequently react with *N*-terminal amino groups as well as lysine, arginine, and cysteine residues in proteins, producing carbamylated proteins (Figure 3) [114]. Given that protein C=O and N-H groups react with the PVDF membrane [34], carbamylation may promote protein adhesion. Furthermore, Tris has been used to stabilize the pH range of cell lysates at 8.5–8.8 [105,107]. Previous studies have used 30 mM [106,107] or 40 mM [105]. We determined the final concentration of urea, thiourea, CHAPS, and Tris in our lysis buffer (Solution C and Solution D, Table 1) based on their various concentrations in previous 2-DE studies.

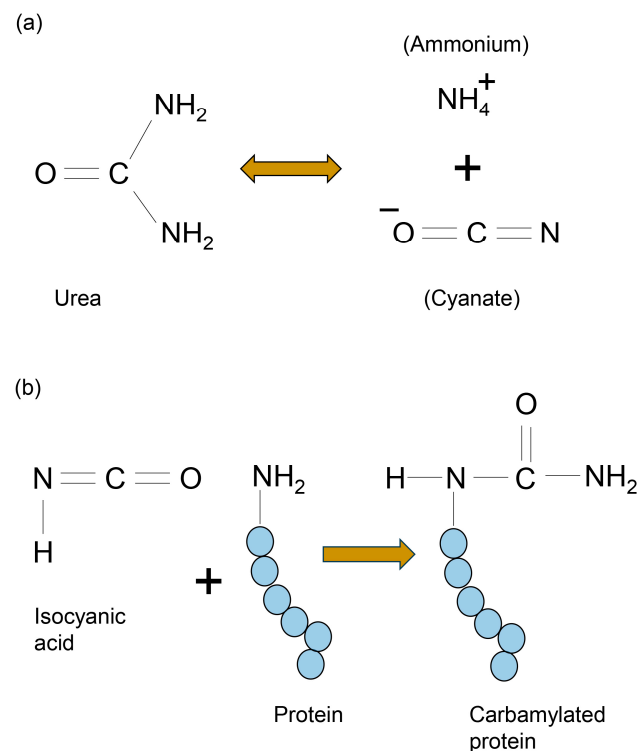


Figure 3. Mechanism of carbamylated protein formation with urea. (a) The reaction path of ammonium and isocyanate from urea. (b) Isocyanic acid attack on *N*-terminal lysine, arginine, and cysteine residues in protein.

We compared each slot blot analysis with different buffers and with nitrocellulose or PVDF membranes (Table 2).

4.4. Application of Standard and Sample Solutions and Vacuum with Water Aspirator

Cell or tissue lysates were prepared with Solution C or Solution D (Table 2) [39,40,90–100]. The protein concentration of the samples was measured using the Bradford method, and equal amounts of cell or tissue lysate (e.g., 2, 4, and 10 μg of protein) were collected [39,40,91–93]. According to the Bio-Rad manufacturing protocol, 200–500 μL of solution should be applied to the membrane; hence, we added 200 μL of the standard or sample solution. Moreover, we diluted each sample with lysate buffer to ensure equal

concentrations [40,91–93]. In our previous study, the volume of the cell or tissue lysate and additional lysis buffer was approximately 4–15 μL , and phosphate-buffered saline (PBS)(–) was added for a final volume of 200 μL . To denature the standard (e.g., AGE-modified protein), it was dissolved in lysis buffer and PBS(–) [39,40,91–93]. The PVDF membrane was activated with methanol before incubation in PBS(–). Three filter papers were then incubated in PBS(–) according to Bio-Rad’s protocol. The PVDF membrane and three filter papers were set in the slot blot apparatus (Figure 4).

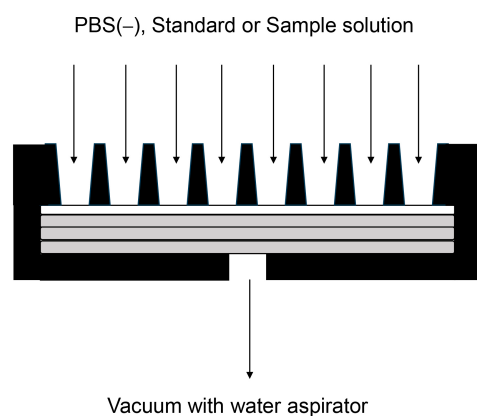


Figure 4. Slot blot apparatus with one PVDF membrane and three filter papers. Chambers are designed for PBS(–), standard and sample solution addition, and vacuum generation. A closed white rectangle represents the PVDF membrane. Closed gray rectangles represent filter papers.

Only the upper side of the PVDF membrane was exposed to air, and PBS(–), standard, and sample solutions were added from the top. The lower side of the PVDF membrane adhered to the filter paper containing the PBS(–). The water aspirator vacuum was applied from the lower side of the PVDF membrane (Figure 4).

The PVDF membrane and filter papers were fixed in the apparatus, and 48 wells were created on the surface of the PVDF membrane (Figure 5). Subsequently, we quantified AGEs using the apparatus [39,90–100].

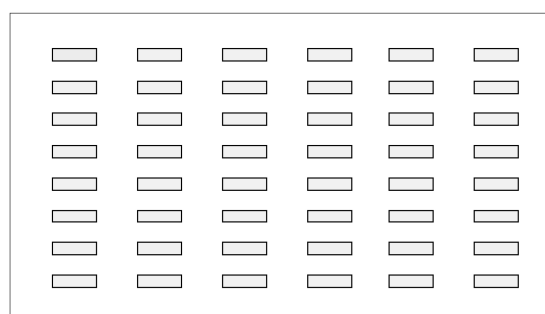


Figure 5. Wells in the slot blot for solution application in the slot blot apparatus. Closed gray squares represent slot lanes.

Before applying the standard or sample solution, the PVDF membrane was washed with PBS(–) according to the Bio-Rad protocol. Accordingly, 100 μL of PBS(–) was added without water aspiration; subsequently, 200 μL of standard or sample solution was added with water aspiration, and one of the valves was opened against the air (Figure 6a). Although the water aspiration pressure was not specified, it was estimated. Water aspirator vacuuming was performed in the Kanazawa Medical University laboratory (Uchinada, Ishikawa, Japan). Water was collected from the water supply, managed with the storage tank, and resupplied to each laboratory. However, the water pressure remained constant,

similar to that of a typical household or corporate water supply system in Uchinada. According to the Ministry of Health, Labour, and Welfare, the feed water pressure is 0.15–0.74 MPa in a typical Japanese household or corporation and 0.20–0.23 MPa in Uchinada. Therefore, all areas of Kanazawa Medical University's water supply system have been adjusted so that their feed water pressure is 0.20–0.23 MPa. For a complete sample addition, we recommend vacuuming with water aspiration with the valve closed against the air (Figure 6b). After adding the standard or sample solution, 200 μ L PBS(–) was applied and vacuumed with water aspiration with one valve opened (Figure 6a) and then closed (Figure 6b) against air. PBS(–) and other solutions were probed onto the PVDF membrane under a water aspirator vacuum, following Bio-Rad's protocols.

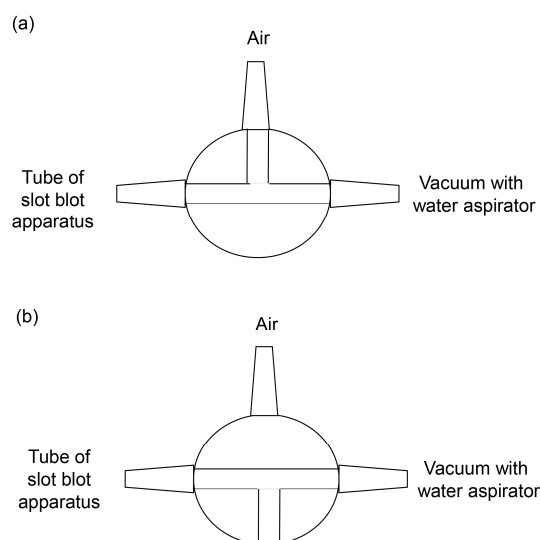


Figure 6. Valve between the slot blot apparatus tube and water aspirator vacuum. (a) The vacuuming with one valve opened against air. (b) The vacuuming with the valve closed against air.

4.5. Protein Quantification in Standard and Sample Solutions

We reported the quantification of certain GA-AGEs [39,90–96,98–100] and 1,5-anhydro-D-fructose AGEs [97] probed with primary antibody, secondary antibody, and chemiluminescent reagents. For example, 0–100 ng/well of standard AGE-modified proteins and approximately 10–20 ng/well (samples with 2.0 μ g of protein were applied onto the PVDF membrane) of AGEs were detected [40,92].

5. Comparing the Novel Slot Blot with Other Slot Blots

Previous studies have reported statistical analysis on data obtained from slot blots performed with a nitrocellulose membrane and RIPA buffer (Table 3) [87,88]. However, those with a PVDF membrane and RIPA buffer did not provide data with error bars and the statistically significant difference [102]. Meanwhile, Gravel et al. presented their data obtained using a PVDF membrane with 4 M urea using error bars without the statistically significant difference [103]. In comparison, data obtained using the novel slot blot was presented with the information of both error bars and the statistically significant difference [39,90–100]. Moreover, we confirmed the suitability of Solutions C and D to promote PVDF membrane probing and facilitate statistical analysis, thus demonstrating the novelty of our assay. Although Papadaki et al. provided data with both error bars and the statistically significant difference [104], they homogenized cardiac tissues with standard rigor buffer containing 1% Triton-X in the first step of the assay and removed Triton-X in the second step. Ultimately, the pellet was resuspended in a buffer containing 8 M urea and 0.1% SDS [104]. Hence, although the data generated from our assay and that of Papadaki et al. were subjected to statistical analysis, our method requires fewer steps to prepare the lysate [39,40,104]. Furthermore, Solution C is suitable to homogenize cells and

tissues. Although this was not confirmed for Solution D, we expect it will be as effective as Solution C.

Table 3. Experimental conditions for slot blot and data analysis.

No.	Sample	Membrane Type	Lysis Buffer	Error Bars	Statistically Significant Difference	References
1	Cell lysate	Nitrocellulose	RIPA	Yes	Yes	[87,88]
2	Cell lysate	PVDF	RIPA	No	No	[102]
3	Protein in virus	PVDF	4 M Urea	Yes	No	[103]
4	Cell lysate	PVDF	Solution C	Yes	Yes	[39,90,92,94–96]
5	Tissue lysate	PVDF	Solution C	Yes	Yes	[91,93]
6	Cell lysate	PVDF	Solution D	Yes	Yes	[97–100]
7	Tissue lysate	PVDF	8 M Urea, 0.1%SDS	Yes	Yes	[104]

6. Potential for Identifying and Quantifying Various Rare Proteins in Kampo Medicines Using the Novel Slot Blot Method

Our novel slot blot method can be used to identify and quantify proteins in Kampo medicines. Compared with test tubes and 96-well microplates, PVDF membrane filtration exhibited particularly good performance. Although the sample volume applied in studies using test tubes and 96-well microplates is typically limited, the slot blot analysis continued until the PVDF membrane became clogged (Figure 4). Hence, one of the slot blot's distinguishing features is that the Kampo medicine extract can be repeatedly dropped onto the PVDF membrane and vacuumed with a water aspirator. Kampo medicines can be extracted with water and collected by removing the water using the freeze-drying method. These samples can be redissolved in Solution C or Solution D (Table 1) and then added to the appropriate PBS(−) solution. Proteins then accumulate on the PVDF membrane as the sample is applied repeatedly (Figures 4 and 5). The accumulation of proteins on the PVDF membrane can then be analyzed using Coomassie Brilliant Blue (CBB) staining (Figure 7), which stains proteins in WB gels [26] and PVDF membranes [116–119]. When WB analysis is performed, samples containing 10–30 µg of protein [26,39,95] are applied to the gel chambers and transferred to the PVDF membrane. When we examined AGEs in kidney tissue, we used a large sample (30 µg of protein) [93]. Researchers can quantify proteins using CBB and our slot blot analysis using a standard curve with 0–100 ng of AGE-modified proteins; in this way, 10–20 ng of AGEs in 2.0 µg of a protein sample can be quantified [92,95,96]. Additionally, this slot blot method may help identify and quantify individual proteins using antibody-based methods such as ELISA (Figure 7) [79–81]. Although our method has risks, such as the binding of polysaccharides to PVDF membranes [120,121], proteins treated with Solution C or D show robust adhesion to the membrane, which could prove advantageous. Bickner et al. identified various proteins probed onto the PVDF membrane using the “on-PVDF membrane digestion” treatment and ESI-MS analysis. The proteins on the membrane were then identified and quantified using the slot blot and ESI-MS/MALDI-MS analysis [38]. However, we consider this strategy to be more challenging than that described by Bickner et al., who performed WB to separate proteins, transferred the proteins onto the PVDF membrane from the gel, and separated them into six groups (the PVDF membrane was cut into six membranes). In contrast, when the slot blot analysis is performed, the proteins are within one area of the PVDF membrane. This is not beneficial for analysis with ESI-MS.

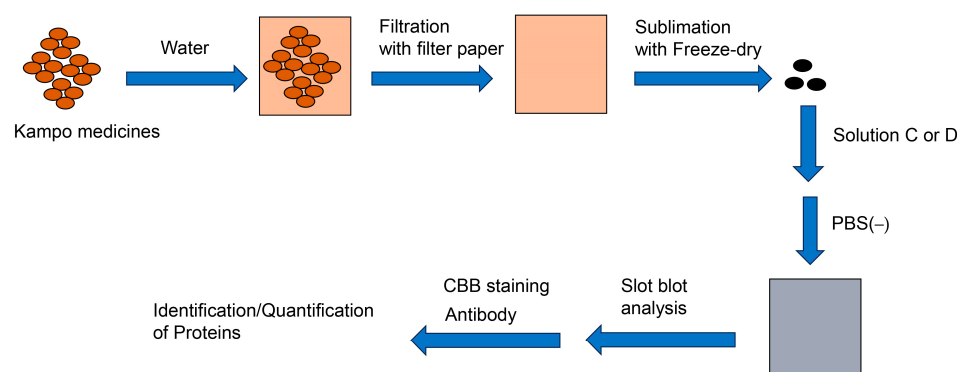


Figure 7. Potential for identifying and quantifying proteins in Kambo medicines. Closed brown circles: Kambo medicine; pale brown square: water extract of Kambo medicine; black circles: pellet samples from the water extract; closed gray square: solution C or D/PBS(−) in which the pellet samples are dissolved.

This study is limited by the absence of confirmatory identification and quantification of the proteins in Kambo medicines using the novel slot blot method. However, we consider that they are able to be detected because AGE-modified proteins in cells and tissue lysates were previously quantified with our slot blot [39,90–100]. Moreover, because the proteins in Kambo medicines should be extracted with high-polarity solvents such as water, any proteins that are not soluble in these solvents will not be detected. Also, we have not confirmed that whole proteins were extracted from Kambo medicines, which requires further verification.

7. Conclusions

Although analysis of rare proteins in Kambo medicines has proven challenging for conventional technology such as column chromatography, WB, and ELISA, methods based on the principle of membrane chromatography, such as slot blot, are effective. We consider that the slot blot analysis is suitable for identifying and quantifying proteins in Kambo medicines because this strategy allows samples to flow continuously without limitation against the membrane. Furthermore, we consider that our novel slot blot, comprising a PVDF membrane and specific lysis buffer, is most suitable as it provides data that show both error bars and the statistically significant difference compared with that produced by other similar assays, and our protocol is simpler, with fewer steps.

Author Contributions: Conceptualization (T.T. and Y.M.), Methodology (T.T. and Y.M.), Writing—Original draft preparation (T.T. and Y.M.), Writing—Review and Editing (T.T., T.M. and Y.M.). All authors have read and agreed to the published version of the manuscript.

Funding: This research was funded by the JSPS KAKENHI, grant number JP21K11607 (T.T.).

Institutional Review Board Statement: Not applicable.

Informed Consent Statement: Not applicable.

Data Availability Statement: The data presented in this study are available in the article.

Conflicts of Interest: The authors declare no conflict of interest.

Abbreviations

AGEs	Advanced glycation end products
CHAPS	3-[(3-cholamidopropyl)-dimethylammonio]-1-propane sulfonate
PBS	Phosphate-buffered saline
PVDF	Polyvinylidene difluoride
Tris	Tris-(hydroxymethyl)-aminomethane
LC	Liquid chromatography

References

1. Chung, H.; Yuasa, M.; Chen, F.; Yukawa, K.; Motoo, Y.; Arai, I. The status of education for integrative medicine in Japanese medical universities with special reference to Kampo medicines. *Tradit. Kampo Med.* **2023**, *10*, 123–131. [[CrossRef](#)]
2. Motoo, Y.; Seki, T.; Tsutani, K. Traditional Japanese medicine, Kampo: Its history and current status. *Clin. J. Integr. Med.* **2011**, *17*, 85–87. [[CrossRef](#)] [[PubMed](#)]
3. Arai, I.; Kawabata, N. Kampo pharmaceutical products in the Japanese health-care system: Legal status and quality assurance. *Tradit. Kampo Med.* **2019**, *6*, 3–11. [[CrossRef](#)]
4. Arai, I. Clinical studies of traditional Japanese herbal medicines (Kampo): Need for evidence by modern scientific methodology. *Integr. Med. Res.* **2021**, *10*, 100722. [[CrossRef](#)] [[PubMed](#)]
5. Motoo, Y.; Hakamatsuka, T.; Kawahara, N.; Arai, I.; Tsutani, K. Standards of Reporting Kampo Products (STORK) in research articles. *J. Integr. Med.* **2017**, *15*, 182–185. [[CrossRef](#)] [[PubMed](#)]
6. Motoo, Y.; Arai, I.; Tsutani, K. Use of Kampo Diagnosis in Randomized Controlled Trials of Kampo Products in Japan: A Systematic Review. *PLoS ONE* **2014**, *9*, e104422. [[CrossRef](#)] [[PubMed](#)]
7. Motoo, Y.; Arai, I.; Kogure, T.; Tsutani, K. Review of the first 20 years Evidence-Based Medicine Committee of the Japan Society for Oriental Medicine. *Tradit. Kampo Med.* **2021**, *8*, 123–139. [[CrossRef](#)]
8. Motoo, Y. Role of Kampo Medicine in Modern Cancer Therapy: Towards Completion of Standard Treatment. *J. Nippon Med. Sch.* **2022**, *89*, 139–144. [[CrossRef](#)]
9. Motoo, Y.; Cameron, S. Kampo medicines for supportive care of patients with cancer: A brief review. *Integr. Med. Res.* **2022**, *11*, 100839. [[CrossRef](#)]
10. Suzuki, T.; Yamamoto, A.; Ohsawa, M.; Motoo, Y.; Mizukami, H.; Makino, T. Effect of ninjin'yoeito and ginseng extracts on oxpliation-induced neuropathies in mice. *J. Nat. Med.* **2017**, *71*, 757–764. [[CrossRef](#)]
11. Sameshima-Uto, N.; Amitani, H.; Atobe, Y.; Sameshima, Y.; Sakaki, M.; Rokot, N.; Ataka, K.; Amitani, M.; Inui, A. Herbal Medicine Ninjin'yoeito in the Treatment of Sarcopenia and Frailty. *Front. Nutr.* **2018**, *5*, 126.
12. Ohnishi, Y.; Fujii, H.; Hayakawa, Y.; Sakukawa, R.; Yamamura, T.; Sakamoto, T.; Tsukada, K.; Fujimaki, M.; Nunome, S.; Komatsu, Y.; et al. Oral Administration of Kampo (Japanese Herbal) Medicine *Juzen-taiho-to* Inhibits Liver Metastastics of Colon 26-L5 Carcinoma Cells. *Jpn. J. Cancer Res.* **1998**, *89*, 206–213. [[CrossRef](#)] [[PubMed](#)]
13. Takagi, K.; Sugihira, T.; Kitamura, M.; Kawai, M.; Mitsuguchi, Y.; Tsukamoto, K.; Nakanishi, H.; Makino, T. Inhibitory effect of Bofutushosan (Fangfengtongshengsan) extract on the absorption of fructose in rats and mice. *J. Nat. Med.* **2023**, *77*, 533–543. [[CrossRef](#)] [[PubMed](#)]
14. Kishida, Y.; Kagawa, S.; Arimitsu, J.; Nakanishi, M.; Sakashita, N.; Otsuka, S.; Yoshikawa, H.; Hagihara, K. Go-sha-jinki-Gan (GJG), a traditional Japanese herbal medicine, protects against in senescence-accelerated mice. *Phytomedicine* **2015**, *22*, 16–22. [[CrossRef](#)] [[PubMed](#)]
15. Nakanishi, M.; Nakae, A.; Kishida, Y.; Baba, K.; Sakashita, N.; Shibata, M.; Yoshikawa, H.; Hagihara, K. Go-sha-jinki-Gan (GJG) ameliorates allodynia in chronic constriction injury model mice via suppression of TNF- α expression in the spinal cord. *Mol. Pain.* **2016**, *12*, 1744806916656382. [[CrossRef](#)] [[PubMed](#)]
16. Hosogi, S.; Ohsawa, M.; Kato, I.; Kuwahara, A.; Inui, T.; Marunaka, Y. Improvement of Diabetes Mellitus Symptoms by Intake of Ninjin'yoeito. *Front. Nutr.* **2018**, *5*, 112. [[CrossRef](#)] [[PubMed](#)]
17. Jin, X.; Uchiyama, M.; Zhang, Q.; Harada, T.; Otsuka, K.; Shimokawa, T.; Niimi, M. Effect of 34 Kinds of Traditional Japanese Herbal Medicines on Prolongation of Cardiac Allograft Survival. *Transplant. Proc.* **2014**, *46*, 1175–1179. [[CrossRef](#)] [[PubMed](#)]
18. Qia, B.L.; Li, Q.L.; Zhang, Y.; Li, K.; Wang, L.; Qiao, Y. Novel Antihypertensive Peptides Derived from Adlay (*Coix lachryma-jobi* L. var. *ma-yuen* Stapf) Glutelin. *Molecules* **2017**, *22*, 123.
19. Lio, B.; Ma, S.; Zhang, S.; Li, X.; Quan, R.; Wan, S. Fructus cannabis protein powder as a green and high effective corrosion inhibitor for Q235 carbon steel in 1 M HCl solution. *Int. J. Biol. Macromol.* **2023**, *239*, 124358. [[CrossRef](#)]
20. Quazi, R.M.; Sajid, Z.; Zhao, C.; Hussain, I.; Ifikhar, F.; Jameel, M.; Rehman, F.U.; Ali, A. Lyophilization Based Isolation of Exosomes. *Int. J. Mol. Sci.* **2023**, *24*, 10477. [[CrossRef](#)]
21. Wang, X.; Ma, Y.; Qi, X.; Ruan, X.; Zhao, F. Practically of non-invasive glucagon-loaded dissolving microneedle for life-saving treatment of severe hypoglycemia in a diabetic rat model. *Int. J. Pharm.* **2023**, *644*, 123340. [[CrossRef](#)] [[PubMed](#)]
22. Armin, V.; Farnaz, M. Practical Techniques for Improving the Performance of Polymeric Membranes and Processes for Protein Separation and Purification. *Iran J. Chem. Chem. Eng.* **2018**, *37*, 1–23.
23. Soxena, A.; Tripathi, B.P.; Kumar, M.; Shahi, V.K. Membrane-based techniques for the separation and purification of proteins: An overview. *Adv. Colloid. Interface Sci.* **2009**, *145*, 1–22. [[CrossRef](#)]
24. Zeng, X.; Ruckenstein, E. Membrane Chromatography: Preparation and Applications to Protein Separation. *Biotechnol. Prog.* **1999**, *15*, 1003–1019. [[CrossRef](#)] [[PubMed](#)]
25. Takata, T.; Hasegawa, T.; Tatsuno, T.; Date, J.; Ishigaki, Y.; Nakamura, N.; Takano, F.; Ohta, T. Isolation of N-acetylneuraminic Acid and N-glycolylneuraminic Acid from *Pleurocybella porrigens*. *J. Health Sci.* **2009**, *55*, 373–379. [[CrossRef](#)]
26. Takata, T.; Ishigaki, Y.; Shimasaki, T.; Tsuchida, H.; Motoo, Y.; Hayashi, A.; Tomosugi, N. Characterization of proteins secreted by pancreatic cancer cells with anticancer drug treatment in vitro. *Oncol. Rep.* **2012**, *28*, 1968–1976. [[CrossRef](#)] [[PubMed](#)]

27. Ahmed, S.; Mahony, C.B.; Torres, A.; Murillo-Saich, J.; Kembel, S.; Cedeno, M.; John, P.; Bhatti, A.; Croft, A.P.; Guma, M. Dual inhibition of glycolysis and glutaminolysis for synergistic therapy of rheumatoid arthritis. *Arthritis Res. Ther.* **2023**, *25*, 176. [[CrossRef](#)]
28. Liu, P.; Tang, W.; Zhao, D.; Zhou, P.; Hu, K. Active metabolites and potential mechanisms of *Notopterygium incisum* against obstructive sleep apnea Syndrome (OSAS): Network analysis and experimental assessment. *Front. Pharmacol.* **2023**, *14*, 1185100. [[CrossRef](#)]
29. Lin, Y.; O'Reilly, M.A.; Hynynen, K. A PVDF Receiver for Acoustic Monitoring of Microbubble-Mediated Ultrasound Brain Therapy. *Sensors* **2023**, *23*, 1369. [[CrossRef](#)]
30. Vierstraete, M.; Beckers, R.; Vangeel, L.; Foriers, B.; Pletinckx, P.; Muysoms, F. Prospective cohort study on mesh shrinkage measured with MRI after robot-assisted minimal invasive retrorectus ventral hernia repair using an iron-oxide-loaded polyvinylidene fluoride mesh. *Surg. Endosc.* **2023**, *37*, 4604–4612. [[CrossRef](#)]
31. Sebastian, L.; Alina, J.; Fabinshy, T.; Dominik, R.; Axel, S.; Jens, H.; Kilian, W.; Cludia, R.; Leonidas, K.; Julia, R.; et al. AbsorbaTack™ vs ProTack™ vs. sutures: A biomechanical analysis of cervical fixation methods for laparoscopic fixations in the porcine model. *Arch. Gynecol. Obstet.* **2023**, *307*, 863–871. [[CrossRef](#)] [[PubMed](#)]
32. Huang, Y.; Cadet, E.R.; King, M.W.; Cole, J.H. Comparison of the mechanical properties and anchoring performance of polyvinylidene fluoride and polypropylene barbed sutures for tendon repair. *J. Biomed. Mater. Res.* **2022**, *110*, 2258–2265. [[CrossRef](#)] [[PubMed](#)]
33. Gao, M.; Zhu, Y.; Yan, J.; Wu, W.; Wang, B. Micromechanism Study of Molecular Compatibility of PVDF/PEI Blend Membrane. *Membranes* **2022**, *12*, 809. [[CrossRef](#)] [[PubMed](#)]
34. Han, M.; Han, Q.; Wu, S.; Xio, H.; Zhang, L.; Lin, Y.; Meng, F.; Zhao, S. Unveiling the Impacts of Sodium Hypochlorite on the Characteristics and Fouling Behaviors of Different Commercial Polyvinylidene Fluoride Hollow Fiber Membranes. *Membranes* **2022**, *12*, 965. [[CrossRef](#)] [[PubMed](#)]
35. Sisay, E.J.; Fazekas, Á.F.; Gyulári, T.; Kopniczky, J.; Hopp, B.; Veréb, G.; Lászó, Z. Investigation of Photocatalytic PVDF Membranes Containing Inorganic Nanoparticles for Model Dairy Wastewater Treatment. *Membranes* **2023**, *13*, 656. [[CrossRef](#)] [[PubMed](#)]
36. Xiang, J.; Wang, S.; Chen, N.; Wen, X.; Tian, G.; Zhang, L.; Cheng, P.; Zhang, J.; Tang, N. Study on Low Thermal-Conductivity of PVDF@SiAG/PET Membranes for Direct Contact Membrane Distillation Application. *Membranes* **2023**, *13*, 773. [[CrossRef](#)] [[PubMed](#)]
37. Ogino, N.; Ogino, K.; Eitoku, M.; Sukanuma, N.; Nagaoka, K. Filter blot method: A simple method for measuring 3-nitrotyrosine in proteins of atmospheric particulate matter. *Environ. Pollut.* **2023**, *329*, 121677. [[CrossRef](#)]
38. Bickner, A.N.; Champion, M.M.; Hummon, A.B.; Bruening, M.L. Electroblothing through a tryptic membrane for LC-MS/MS analysis of proteins separated in electrophoretic gels. *Analyst* **2020**, *145*, 7724–7735. [[CrossRef](#)]
39. Takata, T.; Ueda, T.; Sakasai-sakai, A.; Takeuchi, M. Generation of glyceraldehyde-derived advanced glycation end-products in pancreatic cancer cells and the potential of tumor promotion. *World J. Gastroenterol.* **2017**, *23*, 4910–4919. [[CrossRef](#)]
40. Takata, T. Is the Novel Slot Blot a Useful Method for Quantification of Intracellular Advanced Glycation End-Products? *Metabolites* **2023**, *13*, 564. [[CrossRef](#)]
41. Takata, T.; Motoo, Y. Novel In Vitro Assay of the Effects of Kampo Medicines against Intra/Extracellular Advanced Glycation End-Products in Oral, Esophageal, and Gastric Epithelial Cells. *Metabolites* **2023**, *13*, 878. [[CrossRef](#)] [[PubMed](#)]
42. Phoung-Nguyen, K.; McNeill, B.A.; Aston-Mourney, K.; Rivera, L.R. Advanced Glycation End-Products and Their Effects on Gut Health. *Nutrients* **2023**, *15*, 405. [[CrossRef](#)] [[PubMed](#)]
43. Chen, J.; Radjabzadeh, D.; Medina-Gomez, C.; Voortman, T.; van Merus, J.B.J.; Ikram, M.A.; Uittelinden, A.G.; Kraaij, R.; Zillekens, M.C. Advanced Glycation End Products (AGEs) in Diet and Skin in Relation to Stool Microbiota: The Rotterdam Study. *Nutrients* **2023**, *15*, 2567. [[CrossRef](#)] [[PubMed](#)]
44. Han, D.; Schaffner, S.H.; Davies, J.P.; Benton, M.L.; Plate, L.; Nordman, J.T. BRWD3 promotes KDM5 degradation to maintain H3K4 methylation levels. *Proc. Natl. Acad. Sci. USA* **2023**, *120*, e2305092120. [[CrossRef](#)] [[PubMed](#)]
45. Liu, Z.; Fang, Z.; Wang, K.; Ye, M. Hydrophobic Derivatization Strategy Facilitates Comprehensive Profiling of Protein Methylation. *J. Proteome Res.* **2023**, *22*, 3275–3281. [[CrossRef](#)] [[PubMed](#)]
46. Liu, Y.; Ye, M.; Jang, M.; Chen, X.; Song, G.; Ji, H.; Wang, Z.; Zhu, X. Methylation of BRD4 by PRMT1 regulated BRD4 phosphorylation and promotes ovarian cancer invasion. *Cell Death Dis.* **2023**, *14*, 624. [[CrossRef](#)] [[PubMed](#)]
47. Wang, M.; Gai, X.; Liang, R.; Zhang, E.; Liang, X.; Liang, H.; Fu, C.; Zhou, A.; Shi, Y.; Xu, F.; et al. SIRT1-dependent deacetylation of *Txnip* H3K9ac is critical for exenatide-improved diabetic kidney disease. *Biomed. Pharmacother.* **2023**, *167*, 115515. [[CrossRef](#)]
48. Sun, Q.; Zou, Y.; Feng, Q.; Gong, Z.; Li, M.; Chen, Z. The acetylation of pknH is linked to the ethambutol resistance of *Mycobacterium tuberculosis*. *Arch. Microbiol.* **2023**, *205*, 337.
49. Huang, Z.; Ito, M.; Zhang, S.; Toda, T.; Takeda, J.; Ogi, T.; Ohno, K. Extremely low-frequency electromagnetic field induces acetylation of heat shock proteins and enhances protein folding. *Ecotoxicol. Environ. Saf.* **2023**, *264*, 115482. [[CrossRef](#)]
50. Xiong, H.; Zheng, Z.; Zhao, C.; Zhao, M.; Wang, Q.; Zhang, P.; Li, Y.; Zhu, Y.; Zhu, S.; Li, J. Insight into the underlying molecular mechanisms of dilated cardiomyopathy through integrative analysis of data mining, iTRAQ-PRM proteomics and bioinformatics. *Proteome* **2023**, *21*, 13. [[CrossRef](#)]
51. Toney, N.J.; Schlom, J.; Donahue, R.N. Phosphoflow cytometry to assess cytokine signaling pathways in peripheral immune cell function and treatment response in patients with solid tumors. *J. Exp. Clin. Res.* **2023**, *42*, 247.

52. Chen, D.; Dong, X.; Chen, D.; Lin, J.; Lu, T.; Shen, J.; Ye, H. Chd1 plays a protective role in nonalcoholic fatty liver disease by regulating PPAR/PGC-1 α signaling pathway. *Biochem. Biophys. Res. Commun.* **2023**, *681*, 13–19. [[CrossRef](#)] [[PubMed](#)]
53. Zappi, J.; Tong, Q.; Van der Cruyssen, R.; Cornlis, F.M.F.; Lambert, C.; Coelho, T.P.; Grisart, J.; Kague, E.; Kague, E.; Lories, R.J.; et al. Osteomodulin downregulation is associated with osteoarthritis development. *Bone Res.* **2023**, *11*, 49. [[CrossRef](#)]
54. Mapunda, J.A.; Parejia, J.; Vladymyrov, M.; Bouilet, E.; Hélie, P.; Pleskač, P.; Barcos, S.; Andree, J.; Vesweber, D.; McDonald, D.M.; et al. VE-cadherin in arachoid and pia mater cells serves as a suitable landmark for in vivo imaging of CNS immune surveillance and inflammation. *Nat. Commun.* **2023**, *14*, 5837. [[CrossRef](#)] [[PubMed](#)]
55. Decloquement, M.; Venuto, M.T.; Cogez, V.; Steinmetz, A.; Schulz, C.; Lion, C.; Noel, M.; Rigolot, V.; Teppa, R.E.; Biot, C.; et al. Salmonid polysialyltransferases to generate a variety of sialic acid polymers. *Sci. Rep.* **2023**, *13*, 15610. [[CrossRef](#)] [[PubMed](#)]
56. Maeder, C.; Speer, T.; Wirth, A.; Boeckel, J.; Fatima, S.; Shazad, K.; Freichet, M.; Laufs, U.; Gaul, S. Membrane-bound Interleukin-1 α mediated leukocyte adhesion during atherogenesis. *Front. Immunol.* **2023**, *14*, 1252384. [[CrossRef](#)]
57. Tang, L.; Ye, P.; Yao, L.; Luo, Y.; Tan, W.; Xiang, W.; Liu, Z.; Tan, L.; Xiao, J. LINC01268 promotes epithelial-mesenchymal transition, invasion and metastasis of gastric cancer via the PI3K/Akt signaling pathway and targeting MARCKS. *World J. Gastrointest. Oncol.* **2023**, *15*, 1366–1383. [[CrossRef](#)]
58. Leal, C.S.; Carvalho, C.A.M. In Silico Physicochemical Characterization of Fusion Proteins from Emerging Amazonian Arboviruses. *Life* **2023**, *13*, 1687. [[CrossRef](#)]
59. Jobaer, M.A.; Ashrafi, S.; Asan, M.; Hassan, C.M.; Rashid, M.A.; Ismam, S.N.; Masud, M.M. Phytostemol and Biological Investigation of an Indigenous Plant of Bangladesh, *Gynura procumbens* (Lour.) Merr; Drug Discovery from Nature. *Molecules* **2023**, *28*, 4186. [[CrossRef](#)]
60. Masota, N.; Ohlsen, K.; Schollmayer, C.; Meinei, C.; Holzgrabe, U. Isolation and Characterization of Galloyglucoses Effective against Multidrug-Resistant Strains of *Escherichia coli* and *Klebsiella pneumoniae*. *Molecules* **2022**, *17*, 5045. [[CrossRef](#)]
61. Sananboonodom, S.; Kaewnoi, A.; Pompimon, W.; Narakaew, S.; Jiajaroen, S.; Chainok, K.; Nuntasana, N.; Suksen, K.; Chairoungdua, A.; Limthongkul, J.; et al. Study on the absolute configuration and biological activity of rotenoids, from the leaves and twigs of *Millettia pyrrhocarpa* Mattapha, Forest & Hakins, sp. Nov. *BMC Complement. Med. Ther.* **2023**, *23*, 147.
62. Miyano, K.; Hasegawa, S.; Asai, N.; Uzu, N.; Yatsuoka, W.; Ueno, T.; Nonaka, M.; Uezono, Y. The Japanese Herbal Medicine Hangesshashinto Induce Oral Keratinocyte Migration by Mediating the Expression of CXCL12 Through the Activation of Extracellular Signal-Regulated Kinase. *Front. Pharmacol.* **2022**, *12*, 695039. [[CrossRef](#)]
63. Chung, C.; Lee, M.; Hsia, S.; Chiang, W.; Kuo, Y.; Hsu, H.; Lin, Y. Suppression on allergic inflammation of dehulled adlay (*Coix lachrymal-jobi* L. var. *ma-yuen* Stapf) in mice and anti-degranulation phytosterols from adlay bran. *Food Funct.* **2021**, *12*, 12788–12799. [[CrossRef](#)] [[PubMed](#)]
64. Wang, Y.; Xiong, F.; Zhang, Y.; Wang, S.; Yuan, Y.; Lu, C.; Nie, J.; Nan, T.; Yang, B.; Huang, L.; et al. Application of hyperspectral imaging assistant with integrated deep learning approaches in identifying geographical origins and predicting nutrient contents of Coix seeds. *Food Chem.* **2023**, *404 Pt A*, 134503. [[CrossRef](#)]
65. Sui, Y.; Xu, D. Isolation and identification of anti-inflammatory and analgesic polysaccharides from Coix seed (*Coix lacryma-jobi* L. var. *Ma-yuen* (Roman.) Stapf). *Nat. Prod. Res.* **2022**, *30*, 1–10. [[CrossRef](#)] [[PubMed](#)]
66. Lee, E.; Kim, Y.; Lee, J.; Kim, Y.; Han, K.; Yoon, Y.; Cho, B.; Park, K.; Lee, H.; Cho, J. Comparison of Quality, Antioxidant Capacity, and Anti-Inflammatory Activity of Adlay [*Coix lacryma-jobi* L. var. *ma-yuen* (Rom. Caill.) Stapf.] Sprout at Several Harvest Time. *Plants* **2023**, *12*, 2975. [[PubMed](#)]
67. Tang, X.; Wang, Z.; Zheng, J.; Kan, J.; Chen, G.; Du, M. Physicochemical, Structure properties and in vitro hypoglycemic activity of soluble dietary fiber from adlay (*Coix lacryma-jobi* L. var. *ma-yuen* Stapf) bran treated by steam explosion. *Front Nutr.* **2023**, *10*, 1124012.
68. Huang, Y.; Chen, Y.; Chen, H.; Chiang, Y.; Ali, M.; Chiang, W.; Chung, C.; Hsia, S. Ethanolic Extracts of Adlay Testa Hull and Their Active Biomolecules Exert Relaxing Effects on Uterine Muscle Contraction through Blocking Extracellular Calcium Influx in Ex Vivo and In Vivo Studies. *Biomolecules* **2021**, *11*, 887. [[CrossRef](#)]
69. Chiang, Y.; Chung, C.; Lin, J.; Chiang, W.; Chen, H.; Ali, M.; Shih, Y.; Wang, K.; Huang, T.; Chang, H. Adlay, Seed (*Coix lacryma-jobi* L. var. *Ma-yuen* Stapf.) Ethanolic Extract Fractions and Subfractions Induce Cell Cycle Arrest and Apoptosis in Human Breast and Cervical Cancer Cell Lines. *Molecules* **2022**, *27*, 3984. [[CrossRef](#)]
70. Farinon, B.; Molianari, R.; Costantini, L.; Mereodino, N. The Seed of Industrial Hemp (*Cannabis sativa* L.): Nutritional Quality and Potential Functionality for Human Health and Nutrition. *Nutrients* **2020**, *12*, 1935. [[CrossRef](#)]
71. Chen, N.; Liu, C.; Lin, W.; Ding, Y.; Bian, Z.; Huang, L.; Huang, H.; Yu, K.; Chen, S.; Sun, Y.; et al. Extract of Fructus Cannabis Ameliorates Learning and Memory Impairment Induced by D-Galactose in an Aging Rats Model. *Evid.-Based Complement. Altern. Med.* **2017**, *2017*, 4757520. [[CrossRef](#)] [[PubMed](#)]
72. Iftikhar, A.; Zafar, U.; Ahmed, W.; Shabbir, M.A.; Sameen, A.; Sahar, A.; Bhat, Z.B.; Kowalczewski, P.L.; Jarzębski, M. Applications of *Cannabis sativa* L. in Food and Its Therapeutic Potential: From a Prohibited Drug to a Nutritional Supplement. *Molecules* **2021**, *26*, 7699. [[CrossRef](#)] [[PubMed](#)]
73. Yang, X.; Na, C.; Wang, Y. *Angelica decursiva* exerts antihypertensive activity by inhibiting L-type calcium channel. *J. Ethnopharmacol.* **2023**, *313*, 116527. [[CrossRef](#)]
74. Mihm, A.C.P.; Bonet, L.F.S.; Aiub, C.A.F. Biochemical characterization and phytotoxic activity of protein extract from *Euphorbia tirucalli* L. *J. Ethnopharmacol.* **2022**, *285*, 114903.

75. Moghanloo, S.A.; Forouzanfar, M.; Jafarinia, M.; Fazlollahi, M.R.; Kardar, G.A. Allergen-specific immunotherapy by recombinant Der P1 allergen-derived peptide-based vaccine in an allergic mouse model. *Immun. Inflamm. Dis.* **2023**, *11*, e878. [[CrossRef](#)] [[PubMed](#)]
76. Weber, B.; Stum, R.; Henrich, D.; Marzi, I.; Leppik, L. CD44+ and CD31+ extracellular vesicles (EVs) are significantly reduced in polytraumatized patients with hemorrhagic shock—Evaluation of their diagnostic and prognostic potential. *Front. Immunol.* **2023**, *14*, 1196241. [[CrossRef](#)] [[PubMed](#)]
77. Yong, J.; Hakobyan, K.; Xu, J.; Mellick, A.; Whitelock, J.; Liang, K. Comparison of protein quantification method for protein encapsulation with ZIF-8 metal-organic frameworks. *Biotechnol. J.* **2023**, *12*, e2300015. [[CrossRef](#)]
78. Shegefti, S.; Bolori, S.; Nabavi-Rad, A.; Dabri, H.; Yadegar, A.; Bagaei, K. *Helicobacter pylori*-derived outer membrane vesicles suppress liver autophagy: A novel mechanism for *H. pylori*-mediated hepatic disorder. *Microb. Pathog.* **2023**, *183*, 106319. [[CrossRef](#)]
79. Dai, Y.; Duan, K.; Huang, G.; Yang, X.; Jang, X.; Chen, J.; Liu, P. Inhalation of electronic cigarettes slightly affects lung function and inflammation in mice. *Front. Toxicol.* **2023**, *5*, 1232040. [[CrossRef](#)]
80. Yang, C.; Liu, M.; Peng, Y.; Xu, Z.; Liu, Y.; Guo, Z.; Li, B.; Yang, X. 17 β -estradiol inhibits TGF- β -induced collagen gen contraction mediated by human Tenon fibroblasts via Smads and MAPK signaling pathways. *Int. J. Ophthalmol.* **2023**, *16*, 1441–1449. [[CrossRef](#)]
81. Xing, X.; Wang, H. Correlation of serum HMGB1 and HMGB2 levels with clinical symptoms in allergic rhinitis children. *Medicines* **2023**, *102*, e34921. [[CrossRef](#)] [[PubMed](#)]
82. Kumar, S.; Zheng, H.; Deng, B.; Mahajan, B.; Grabias, B.; Kozakai, Y.; Morin, M.J.; Locke, E.; Birkett, A.; Miura, K.; et al. A Slot Blot Immunoassay for Quantitative Detection of *Plasmodium falciparum* Circumsporozoite Protein in Mosquito Midgut Oocyst. *PLoS ONE* **2014**, *9*, e115807. [[CrossRef](#)] [[PubMed](#)]
83. Grabias, B.; Verma, N.; Zheng, H.; Tripathi, A.K.; Mlambo, G.; Morin, M.J.; Locke, E.; Kumar, S. A no film slot blot for the detection of developing *P. falciparum* oocysts in mosquitoes. *PLoS ONE* **2017**, *12*, e0174229. [[CrossRef](#)] [[PubMed](#)]
84. Ghiani, A.; Ania, R.; Asero, R.; Bellotto, E.; Citterio, S. Ragweed pollen collected along high-traffic roads shows a higher allergenicity than pollen sampled in vegetated areas. *Allergy* **2012**, *67*, 887–894. [[CrossRef](#)] [[PubMed](#)]
85. Nimmo, J.T.; Verma, A.; Dodart, J.-C.; Wang, C.Y.; Savistchenko, J.; Melki, R.; Carare, R.O.; Nicoll, J.A.R. Novel antibodies detect additional α -synuclein pathology in synucleinopathies: Potential development for immunotherapy. *Alzheimer's Res. Ther.* **2020**, *12*, 159. [[CrossRef](#)]
86. Barandalla, M.; Haucke, E.; Fischer, B.; Santos, A.N.; Colleoni, S.; Galli, C.; Santos, A.N.; Lazzari, G. Comparative Analysis of AGE and RAGE Levels in Human Somatic and Embryonic Stem Cell under H₂O₂-Induced Noncytotoxic Oxidative Stress Conditions. *Oxid. Med. Cell. Longev.* **2017**, *2017*, 4240136. [[CrossRef](#)]
87. Koriyama, Y.; Furukawa, A.; Muramatsu, M.; Takino, J.; Takeuchi, M. Glyceraldehyde caused Alzheimer's disease-like alterations in diagnostic marker levels in SH-SY5Y human neuroblastoma cells. *Sci. Rep.* **2015**, *5*, 13313. [[CrossRef](#)]
88. Nasu, R.; Furukawa, A.; Suzuki, K.; Takeuchi, M.; Koriyama, Y. The Effect of Glyceraldehyde-Derived Advanced Glycation End Products on β -Tubulin-Inhibited Neurite Outgrowth in SH-SY5Y Human Neuroblastoma Cells. *Nutrients* **2020**, *12*, 2958. [[CrossRef](#)]
89. Kumar, S.T.; Jagannath, S.; Francois, C.; Vanderstichele, H.; Stoops, E.; Lashuel, H.A. How specific are the conformation-specific α -synuclein antibodies? Characterization and validation of 16 α -synuclein conformation-specific antibodies using well-characterized preparations of α -synuclein monomers, fibrils and oligomers with distinct structures and morphology. *Neurobiol. Dis.* **2020**, *146*, 10586.
90. Takata, T.; Sakasa-Sakai, A.; Ueda, T.; Takeuchi, M. Intracellular toxic advanced glycation end-products in cardiomyocytes may cause cardiovascular disease. *Sci. Rep.* **2019**, *9*, 2121. [[CrossRef](#)]
91. Takata, T.; Sakasa-Sakai, A.; Takino, J.; Takeuchi, M. Evidence for Toxic Advanced Glycation End-Products Generated in the Normal Rat Liver. *Nutrients* **2019**, *11*, 1612. [[CrossRef](#)] [[PubMed](#)]
92. Takata, T.; Sakasa-Sakai, A.; Takeuchi, M. Impact of intracellular toxic advanced glycation end-products (TAGE) on murine myoblast cell death. *Diabetol. Metab. Syndr.* **2020**, *12*, 54. [[CrossRef](#)] [[PubMed](#)]
93. Inoue, S.; Takata, T.; Nakazawa, Y.; Nakamura, Y.; Guo, X.; Yamada, S.; Ishigaki, Y.; Takeuchi, M.; Miyazawa, K. Potential of an Interorgan Network Mediated by Toxic Advanced Glycation End-Products in a Rat Model. *Nutrients* **2021**, *13*, 80. [[CrossRef](#)] [[PubMed](#)]
94. Kikuchi, C.; Sakasa-Sakai, A.; Okimura, R.; Tanaka, H.; Takata, T.; Takeuchi, M.; Matsunaga, T. Accumulation of Toxic Advanced Glycation End-Products Induces Cytotoxicity and Inflammation in Hepatocyte-Like Cells Differentiated from Human Induced Pluripotent Stem Cells. *Biol. Pharm. Bull.* **2021**, *44*, 1399–1402. [[CrossRef](#)] [[PubMed](#)]
95. Takata, T.; Sakasa-Sakai, A.; Takeuchi, M. Intracellular Toxic Advanced Glycation End-Products in 1.4E7 Cell Line Induce Death with Reduction of Microtubule-Associated Protein 1 Light Chain 3 and p62. *Nutrients* **2022**, *14*, 332. [[CrossRef](#)] [[PubMed](#)]
96. Takata, T.; Sakasa-Sakai, A.; Takeuchi, M. Intracellular Toxic Advanced Glycation End-Products May Induce Cell Death and Suppress Cardiac Fibroblasts. *Metabolites* **2022**, *12*, 615. [[CrossRef](#)] [[PubMed](#)]
97. Sakasa-Sakai, A.; Takata, T.; Suzuki, H.; Maruyama, I.; Motomiya, Y.; Takeuchi, M. Immunological evidence for in vivo production of novel advanced glycation end-products from 1,5-anhydro-D-fructose, a glycogen metabolite. *Sci. Rep.* **2019**, *9*, 10194. [[CrossRef](#)] [[PubMed](#)]

98. Sakasai-Sakai, A.; Takata, T.; Takeuchi, M. Intracellular Toxic Advanced Glycation End-Products Promote the Production of Reactive Oxygens Species in HepG2 Cells. *Int. J. Mol. Sci.* **2020**, *21*, 4861. [[CrossRef](#)]
99. Sakasai-Sakai, A.; Takata, T.; Takeuchi, M. The Association between Accumulation of Toxic Advanced Glycation End-Products and Cytotoxic Effect in MC3T3-E1 Cells. *Nutrients* **2022**, *14*, 990. [[CrossRef](#)]
100. Sakasai-Sakai, A.; Takata, T.; Takino, J.; Takeuchi, M. Impact of intracellular glyceraldehyde-derived advanced glycation end-products on human hepatocyte cell death. *Sci. Rep.* **2017**, *7*, 14282. [[CrossRef](#)]
101. Browicka-Szydelko, A.; Krzystek-Korpacka, M.; Kuzan, A.; Gostomaska-Pampuch, K.; Gacka, M.; Jakobsche-Policht, U.; Adamiec, R.; Gamian, A. Non-standard AGE4 epitopes that predict polyneuropathy independently of obesity can be detected by slot dot-blot immunoassay. *Adv. Clin. Exp. Med.* **2020**, *29*, 91–100. [[CrossRef](#)] [[PubMed](#)]
102. Takino, J.; Kobayashi, Y.; Takeuchi, M. The formation of intracellular glyceraldehyde-derived advanced glycation end-products and cytotoxicity. *J. Gastroenterol.* **2010**, *45*, 646–653. [[CrossRef](#)] [[PubMed](#)]
103. Gravel, C.; Li, C.; Wang, J.; Hashem, A.M.; Jaentschke, B.; van Domselaar, G.; He, R.; Li, X. Quantitative Analyses of all Influenza Type A Viral Hemagglutinins and Neuraminidases using Universal Antibodies in Simple Slot Blot Assays. *J. Vis. Exp.* **2011**, *4*, 2784.
104. Papadaki, M.; Holewinski, R.J.; Previs, S.B.; Martin, T.G.; Stachowski, M.J.; Li, A.; Blair, C.A.; Morave, C.S.; Van Eyk, J.E.; Campbell, K.S.; et al. Diabetes with heart failure increases methylglyoxal modifications in the sarcomere, which inhibit function. *JCI Insight* **2018**, *3*, e121264. [[CrossRef](#)] [[PubMed](#)]
105. Gil-Agusti, M.T.; Campostrini, N.; Zolla, L.; Ciambella, C.; Invernizzi, C.; Righetti, G. Two-dimensional mapping as a tool for classification of green coffee bean species. *Proteomics* **2005**, *5*, 710–718. [[CrossRef](#)] [[PubMed](#)]
106. Cui, Y.; Tian, M.; Zong, M.; Teng, M.; Chen, Y.; Lu, J.; Jiang, J.; Liu, X.; Han, J. Proteomics Analysis of Pancreatic Ductal Adenocarcinoma Compared with Normal Adjacent Pancreatic Tissue and Pancreatic Benign Cystadenoma. *Pancreatology* **2009**, *9*, 89–98. [[CrossRef](#)] [[PubMed](#)]
107. Sakolvaree, Y.; Maneewatch, S.; Jiemsup, S.; Klaysing, B.; Tongtawe, P.; Srimanote, P.; Saengjaruk, P.; Banyen, S.; Tapchaisri, P.; Chonsa-nguan, M.; et al. Proteome and Immunome of Pathogenic *Leptospira* spp. Revealed by 2DE and 2DE-Immunoblotting with Immune Serum. *Asian Pac. J. Allergy Immunol.* **2007**, *25*, 53–73.
108. Twine, S.M.; Mykytczuk, N.C.S.; Petit, M.; Tremblay, T.; Conlan, J.W.; Kelly, J.F. *Francisella tularensis* Proteome: Low Levels of ASB-14 Facilitate the Visualization of Membrane Proteins in Total Protein Extracts. *J. Proteome Res.* **2005**, *4*, 1848–1854. [[CrossRef](#)]
109. Wu, Y.; Zhou, J.; Zhang, X.; Zheng, X.; Jiang, X.; Shi, L.; Yin, W.; Wang, J. Optimized samples preparation for two-dimensional gel electrophoresis of soluble proteins from chicken bursa of Fabricus. *Proteome Sci.* **2009**, *7*, 38. [[CrossRef](#)]
110. Campos, A.; Puetro, M.; Prieto, A.; Cameán, A.; Almeida, A.M.; Coelho, A.; Vasconcelos, V.J. Protein extraction and two-dimensional gel electrophoresis of proteins in the marine mussel *Mytilus galloprovincialis*: An important tool for protein expression studies, food quality and safety assessment. *Sci. Food Agric.* **2013**, *93*, 1779–1787. [[CrossRef](#)]
111. Pedroso, A.P.; Watanabe, R.L.H.; Albuquerque, K.T.; Telles, M.M.; Andrade, M.C.C.; Perez, J.D.; Sakata, M.M.; Lima, M.L.; Estadella, D.; Nascimento, C.M.O.; et al. Proteomic profiling of the rat hypothalamus. *Proteome Sci.* **2012**, *10*, 26. [[CrossRef](#)] [[PubMed](#)]
112. Farinazzo, A.; Fasoli, E.; Kravchuk, A.V.; Candiano, G.; Aldini, G.; Regazzoni, L.; Righetti, P.G. En bloc elution of proteomes from combinatorial peptide ligand libraries. *J. Proteom.* **2009**, *72*, 725–730. [[CrossRef](#)] [[PubMed](#)]
113. Herbert, B. Advances in protein solubilization for two-dimensional electrophoresis. *Electrophoresis* **1999**, *20*, 660–663. [[CrossRef](#)]
114. McCarthy, J.; Hopwood, F.; Oxley, D.; Laver, M.; Castagna, A.; Righetti, P.G.; Williams, K.; Herbert, B. Carbamylation of Protein in 2-D Electrophoresis—Myth or Reality? *J. Proteome Res.* **2003**, *2*, 239–242. [[CrossRef](#)] [[PubMed](#)]
115. Tit-Oon, P.; Chokchaichamnankit, D.; Khongmanee, A.; Sawangretrakul, P.; Svasti, J.; Srisomsap, C. Comparative secretome analysis of cholangiocarcinoma cell line in three-dimensional culture. *Int. J. Oncol.* **2014**, *45*, 2108–2116. [[CrossRef](#)] [[PubMed](#)]
116. Shimazaki, Y.; Michhiro, M. Analysis of trypsin inhibition activity in human plasma proteins after separation by non-denaturing two-dimensional electrophoresis. *Clin. Chim. Acta* **2013**, *425*, 48–53. [[CrossRef](#)] [[PubMed](#)]
117. Kawasaki, H.; Okayama, A.; Iwafune, Y.; Yahagi, S.; Arakawa, N.; Hirano, H. Multiplex detection and identification of proteins on a PVDF membrane blocked with a synthetic polymer-based reagent. *Electrophoresis* **2008**, *29*, 4377–4380. [[CrossRef](#)]
118. Nie, X.; Li, C.; Hu, S.; Xue, F.; Kang, J.; Zhang, W. An appropriate loading control for western blot analysis in animal model of myocardial ischemic infarction. *Biochem. Biophys. Res.* **2017**, *12*, 108–113. [[CrossRef](#)]
119. Kurien, B.; Scefild, R.H. A brief review of other notable protein blotting methods. *Methods Mol. Biol.* **2009**, *536*, 367–384.
120. Taoerdalhong, H.; Zhou, K.; Yang, F.; Dong, C. Structure, immunostimulatory activity, and the effect of ameliorating airway inflammation of polysaccharides from *Pyrus sinkiangensis* Yu. *Int. J. Biol. Macromol.* **2022**, *195*, 246–254. [[CrossRef](#)]
121. Huang, C.; Peng, X.; Pang, D.; Li, J.; Paulsen, B.S.; Eise, F.; Chen, Y.; Chen, Z.; Jia, R.; Li, L. Pectic polysaccharide from *Nelumbo nucifera* leaves promotes intestinal antioxidant defense in vitro and in vivo. *Food Funct.* **2021**, *12*, 10828–10841. [[CrossRef](#)] [[PubMed](#)]

Disclaimer/Publisher’s Note: The statements, opinions and data contained in all publications are solely those of the individual author(s) and contributor(s) and not of MDPI and/or the editor(s). MDPI and/or the editor(s) disclaim responsibility for any injury to people or property resulting from any ideas, methods, instructions or products referred to in the content.